PROCEEDINGS OF SCIENCE

The proton form factor ratio results from Jefferson Lab

Vina Punjabi*
Norfolk State University, Norfol, Va 23504, USA
E-mail: vapunjabi@nsu.edu

The ratio of the proton form factors, G_{Ep}/G_{Mp}, has been measured extensively, from Q^2 of 0.5 GeV^2 to 8.5 GeV^2, at the Jefferson Laboratory, using the polarization transfer method. This ratio is extracted directly from the measured ratio of the transverse and longitudinal polarization components of the recoiling proton in elastic electron-proton scattering. The polarization transfer results are of unprecedented high precision and accuracy, due in large part to the small systematic uncertainties associated with the experimental technique. There is an approved experiment at JLab, GEP(5), to continue the ratio measurements to 12 GeV^2. A dedicated experimental setup, the Super Bigbite Spectrometer (SBS), will be built for this purpose. It will be equipped with a focal plane polarimeter to measure the polarization of the recoil protons. The scattered electrons will be detected in an electromagnetic calorimeter. In this presentation, I will review the status of the proton elastic electromagnetic form factors and discuss a number of theoretical approaches to describe nucleon form factors.

Sixth International Conference on Quarks and Nuclear Physics
April 16-20, 2012
Ecole Polytechnique, Palaiseau, Paris

*Speaker.

PoS(QNP2012)034

One of the fundamental goals of nuclear physics is to understand the structure and behavior of strongly interacting matter in terms of its basic constituents, quarks and gluons. An important step towards this goal is the characterization of the internal structure of the nucleon. The elastic electromagnetic form factors are directly related to the charge and current distributions inside the nucleon; these form factors are among the most basic observables of the nucleon.

The two Sachs form factors, G_{Ep} and G_{Mp}, have been measured extensively over the last several decades using two experimental techniques; one, the Rosenbluth separation method [1], and second, the polarization transfer method [2, 3].

In the one photon exchange approximation, the Sachs form factors depend only upon the four-momentum squared, Q^2, of the reaction. The elastic *ep* cross section in terms of the Sachs form factors can be expressed as:

$$\frac{d\sigma}{d\Omega} = \frac{\alpha^2\, E'_e\, \cos^2\frac{\theta_e}{2}}{4E_e^3\, \sin^4\frac{\theta_e}{2}} \left[G_{Ep}^2 + \frac{\tau}{\varepsilon} G_{Mp}^2\right] \left(\frac{1}{1+\tau}\right), \tag{1}$$

where $\tau = Q^2/4M^2$ and ε is the virtual photon longitudinal polarization, $\varepsilon = [1+2(1+\tau)\tan^2(\frac{\theta_e}{2})]^{-1}$, M is the mass of the proton.

In Rosenbluth method, the separation of G_{Ep}^2 and G_{Mp}^2 is achieved by fitting data with a straight line fit at a given Q^2 over a range of ε obtained by changing the beam energy, E_e and electron scattering angle, θ_e. The form factors, G_{Ep} and G_{Mp}, obtained from all cross section measurements are shown in Fig. 1 and 2; they have been divided by the dipole form factor $G_D = (1+\frac{Q^2}{0.71})^{-2}$. Evidently the form factors divided by G_D appear to remain close to 1. This behavior suggested that G_{Ep}, and G_{Mp} have similar spatial distributions.

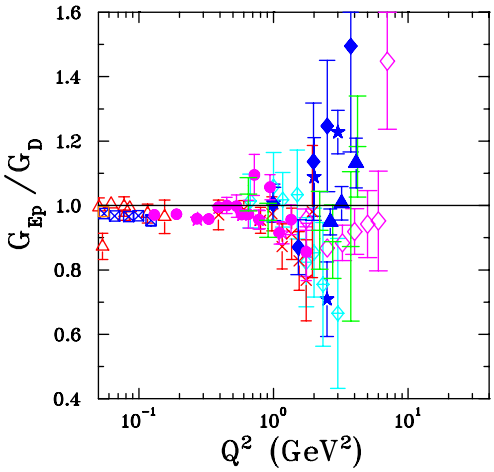

Figure 1: World data base for G_{Ep} obtained by the Rosenbluth method.

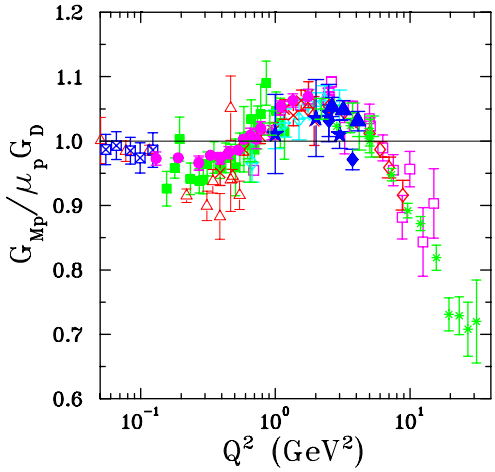

Figure 2: World data base for G_{Mp} obtained by the Rosenbluth method.

In the one-photon exchange approximation, in the $\vec{e}p \rightarrow e\vec{p}$ reaction, the scattering of longitudinally polarized electrons results in a transfer of polarization to the recoil proton with only two non-zero components, P_t perpendicular to, and P_ℓ parallel to the proton momentum in the scattering plane. For 100 % longitudinally polarized electrons, the polarizations are [2, 3]:

$$I_0 P_n = 0 \tag{2}$$

$$I_0 P_t = -2\sqrt{\tau(1+\tau)} G_{Ep} G_{Mp} \tan\frac{\theta_e}{2} \tag{3}$$

$$I_0 P_\ell = \frac{1}{M_p}(E_{beam}+E_e)\sqrt{\tau(1+\tau)} G_{Mp}^2 \tan^2\frac{\theta_e}{2} \tag{4}$$

where I_0 is proportional to the unpolarized cross section and is given by:

$$I_0 = G_{Ep}^2 + \frac{\tau}{\varepsilon} G_{Mp}^2 \tag{5}$$

Eqs. (3) and (4) show that $I_o P_t$ and $I_o P_\ell$ are proportional to $G_{Ep}G_{Mp}$ and G_{Mp}^2, respectively. Together these equations give:

$$\frac{G_{Ep}}{G_{Mp}} = -\frac{P_t}{P_\ell}\frac{(E_{beam}+E_e)}{2M_p}\tan\frac{\theta_e}{2} \tag{6}$$

The ratio G_{Ep}/G_{Mp} is obtained from a single measurement of the two recoil polarization components P_t and P_ℓ in a polarimeter, whereas the Rosenbluth method requires at least two cross section measurements made at different energy and angle combinations at the same Q^2.

The unexpected result from JLab shown in Fig. 3, using the polarization transfer technique to measure the proton electric over magnetic form factor ratio, G_{Ep}/G_{Mp} [4, 5, 6, 7], has been the revelation that the form factors obtained using the polarization and Rosenbluth separation methods [8, 9, 10], were incompatible with each other, starting around $Q^2 = 3$ GeV^2 The form factors obtained from cross section data had suggested that $G_{Ep} \sim G_{Mp}/\mu_p$, where μ_p is the proton magnetic moment; the results obtained from recoil polarization data clearly show that the ratio G_{Ep}/G_{Mp} decreases linearly with increasing momentum transfer Q^2. The results seen in Fig. 3 suggest that the spatial distribution of the electric charge of the proton is "softer", *i.e.*, larger in extent (in the Breit frame) than its magnetization currents distribution, which is definitively not intuitive. However, the relativistic boost required to transform these spatial distributions back to the laboratory frame are not trivial and only the form factors themselves are the relativistic invariants. Recently, G.A. Miller [11] has shown that a model independent charge distribution can only be defined on the wave front; the two-dimensional charge density on the wave-front is the Fourier transform of the Dirac form factor, F_1.

These striking results for the proton electromagnetic form factor ratio obtained through double polarization experiments, have put the field of nucleon elastic electromagnetic form factors into the limelight, giving it a new life.

Predicting nucleon form factors in the non-perturbative regime, where soft scattering processes are dominant, is very difficult. As a consequence there are many phenomenological models which attempt to explain the data in this domain; precise measurements of the nucleon form factors are necessary to constrain and test these models.

There are several approaches to calculate nucleon form factors in the non-perturbative regime. The list includes vector meson dominance (VMD) models [12, 13], relativistic constituent quark models (rCQM) [14, 15, 16, 17, 18, 19], the cloudy bag model, the di-quark model and the Dyson-Schwinger equation (DSE) [20] model and more. In the VMD approach, the photon couples to the

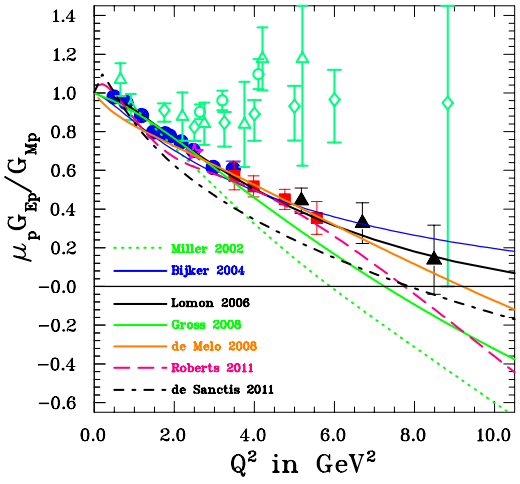

Figure 3: Recoil polarization results for $\mu_p G_{Ep}/G_{Mp}$ from four JLab experiments; also included are selected Rosenbluth results (green empty diamonds). Theoretical predictions from several different models are shown.

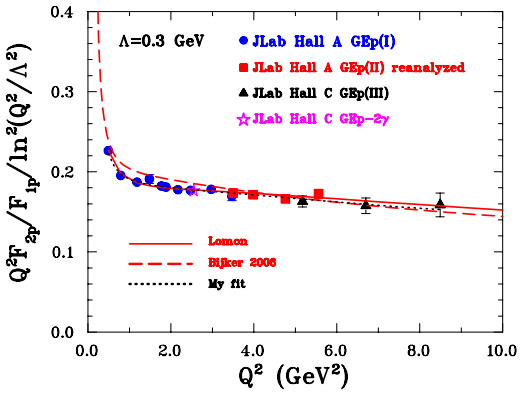

Figure 4: The test of the modified scaling prediction for Q^2F_{2p}/F_{1p} versus Q^2 [24] for data from four JLab experiments.

nucleon via vector mesons, whereas in QCD models the photon couples to the quarks directly. The generalized parton distributions (GPD) [21, 22] represent a framework within which hadrons are described in terms of quarks and gluons. Perturbative QCD [23, 24] predicts form factor values for large Q^2. We show results from some of these calculations here in Fig. 3.

In the pQCD approach proposed by Brodsky and collaborators [23], Q^2F_{2p}/F_{1p} should become constant at very high Q^2. The results from four JLab experiments disagree with this prediction. In another approach, it has been shown in Ref. [24] that by including components in the nucleon light-cone wave functions with quark orbital angular momentum projection $l_z = 1$, one obtains the behavior $Q^2F_2/F_1 \rightarrow \ln^2(Q^2/\Lambda^2)$ at large Q^2, with Λ a non-perturbative mass scale. Choosing Λ around 0.3 GeV, Ref. [24] noticed that the data for Q^2F_{2p}/F_{1p} support such double-logarithmic enhancement, as can be seen from Figure 4.

The matrix element of the hadronic current in elastic ep scattering is of the form $< N|e_u\bar{u}\gamma_\mu u + e_d\bar{d}\gamma_\mu d|N >$, where N stands for a nucleon, and e_u and e_d are the charge of the u and d "dressed" quarks, respectively; and with the further assumption of isospin symmetry for the corresponding u and d quark $F_{1p,n}^{u,d}$ and $F_{2p,n}^{u,d}$ form factors, implying:

$$F_{1n}^d = F_{1p}^u \text{ and } F_{1n}^u = F_{1p}^d,$$

and similar relations for F_2, the flavor separated u and d quark form factors in the nucleons are linear combinations of the measured form factors $F_{1p,n}$ and $F_{2p,n}$:

$$F_1^u = 2F_{1p} + F_{1n} \text{ and } F_1^d = F_{1p} + 2F_{1n},$$

$$F_2^u = 2F_{2p} + F_{2n} \text{ and } F_2^d = F_{2p} + 2F_{2n}.$$

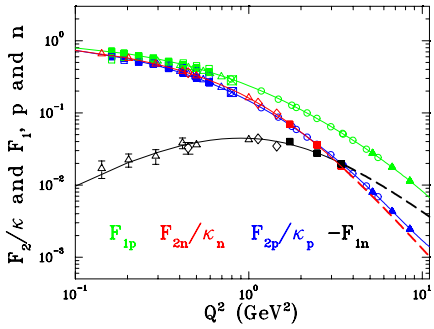

Figure 5: the Dirac and Pauli form factors of proton and neutron, as obtained from the data $\mu G_E/G_M$ with a polynomial fit.

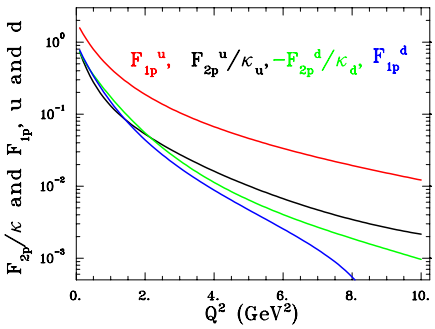

Figure 6: The separated *u* and *d* quark form factors corresponding to the curves in Fig. 5, and assuming isospin symmetry.

A similar flavor separation was recently published by Cates et al [25]. Here we use our own fit shown in Fig. 5 to $F_{1p,1n}$ and $F_{2p,2n}$ to get a more general view of these flavor separated form factors. Remarkable is the similar Q^2-dependence of three of these form factors as seen in Fig. 6, the exception is F_1^u, which is twice as large as the others at Q^2=0, as expected, but may become 10 times larger than the three others at 10 GeV^2. The neutron data base stops at 3.4 GeV^2, so these curves are to be taken as a possibility, supported by the smooth behavior and excellent agreement of the Dirac and Pauli form factor demonstrated in Fig. 5 over the region of Q^2 where data exist.

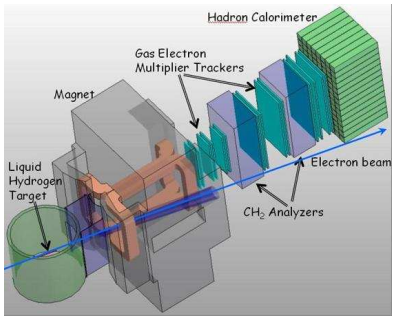

Figure 7: Schematic of the super bigbite spectrometer.

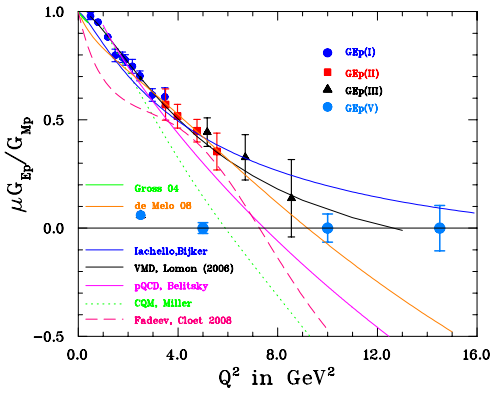

Figure 8: The anticipated results of GEp(5).

The higher design energy of JLab 12 GeV will give access to higher momentum transfers in all form factor measurements, in the Q^2 range 10 to 20 GeV^2. Super Bigbite Spectrometer (SBS) shown in Fig. 7 is a large-acceptance spectrometer, based on the Super Bigbite magnet, that will incorporate a focal plane and a double polarimeter instrumented with GEM trackers and a highly-segmented hadron calorimeter. The GEp(5) experiment will use SBS to detect recoil protons, and a large solid angle electromagnetic calorimeter to detect scattered electrons, in coincidence with recoiling proton. In Fig. 8 anticipated results of GEp(5) are shown with A wide range of

phenomenological model predictions, underlining the potential ability of this experiment, to narrow the range of models able to reproduce the future data.

References

[1] M.N. Rosenbluth, Phys. Rev. **79**, 615 (1950).

[2] A. I. Akhiezer and M. P. Rekalo, Sov. J. Part. Nucl. **4**, 277 (1974);Fiz. Elem. Chast. Atom. Yadra **4**, 662 (1973).

[3] R.G. Arnold, C.E. Carlson, F. Gross, Phys. Rev. C **23**, 363 (1981).

[4] M.K. Jones *et al.*, Phys. Rev. Lett. **84**, 1398 (2000); V. Punjabi *et al.*, Phys. Rev. C **71** 055202 (2005).

[5] O. Gayou *et al.*, Phys. Rev. Lett. **88** 092301 (2002); A.J.R. Puckett *et al.*, Phys. Rev. C **85**, 045203 (2012).

[6] A.J.R. Puckett *et al.*, Phys. Rev. Lett., **104**, 242307 (2010).

[7] M. Meziane *et al.* [GEp2gamma Collaboration], Phys. Rev. Lett. **106**, 132501 (2011).

[8] L. Andivahis *et al.* Phys. Rev. D **50** 5491 (1994).

[9] M.E. Christy *et al.*, Phys. Rev. C **70** 015206 (2004).

[10] I.A. Qattan *et al.*, Phys. Rev. Lett. **94**, 142301 (2005).

[11] G.A. Miller, arXiv:0705.2409 (2007); Phys. Rev. Lett. **99**, 112001 (2007).

[12] E.L. Lomon, Phys. Rev. C **64**, 035204 (2001), Phys. Rev. C**66**, 045501 (2002) and arXiv:nucl-th/0609020 (2006).

[13] R. Bijker and F. Iachello, Phys. Rev. C **69**, 068201 (2004).

[14] M.R. Frank, B.K. Jennings, and G.A. Miller, Phys. Rev. C **54**, 920 (1996); G.A. Miller and M.R. Frank, Phys. Rev. C **65**, 065205 (2002).

[15] Cardarelli F. and S. Simula, Phys. Rev. C **62**, 65201 (2000).

[16] S. Boffi *et al.*, Eur. Phys. J. A **14**, 17 (2002).

[17] F. Gross and P. Agbakpe, Phys. Rev. C **73**, 015203 (2006); F. Gross, G. Ramalho and M. T. Pena, Phys. Rev. C **77**, 015202 (2008).

[18] J.P.B. de Melo, T. Frederico, E. Pace, S. Pisano and G. Salme, arXiv:0804.1511 [hep-ph] (2008).

[19] M. De Sanctis, J. Ferretti, E. Santopinto and A. Vassallo, Phys. Rev. C **84**, 055201 (2011).

[20] I.C. Cloët, G. Eichmann, B. El-Bennich, T. Klähn and C.D. Roberts, arXiv:0812.0416 [nucl-th] (2008).

[21] X. Ji, Phys. Rev. D **55**, 7114 (1997); Phys. Rev. Lett. **78** 610 (1997).

[22] M. Guidal, M.V. Polyakov, A.V. Radyushkin and M. Vanderhaeghen, Phys. Rev. D **72**, 054013 (2005).

[23] S. Brodsky and G.R. Farrar, Phys. Rev. D **11**, 1309 (1975).

[24] A.V. Belitsky, X. Ji and F. Yuan, Phys. Rev. Lett. **91**, 092003 (2003).

[25] G.D. Cates, C.W. de Jager, S. Riordan and B. Wojtsekhowski, Phys. Rev. Lett. **106**, 252003 (2011).